

Podoplanin-Fc reduces lymphatic vessel formation in vitro and in vivo and causes disseminated intravascular coagulation when transgenically expressed in the skin

Leah N. Cueni,¹ Lu Chen,² Hui Zhang,² Daniela Marino,¹ Reto Huggenberger,¹ Annamari Alitalo,¹ Roberta Bianchi,¹ and Michael Detmar¹

¹Institute of Pharmaceutical Sciences, Swiss Federal Institute of Technology, ETH Zurich, Zurich, Switzerland; and ²Center for Eye Disease and Development, Program in Vision Science and School of Optometry, University of California at Berkeley, Berkeley, CA

Podoplanin is a small transmembrane protein required for development and function of the lymphatic vascular system. To investigate the effects of interfering with its function, we produced an Fc fusion protein of its ectodomain. We found that podoplanin-Fc inhibited several functions of cultured lymphatic endothelial cells and also specifically suppressed lymphatic vessel growth, but not blood vessel growth, in mouse embryoid bodies in vitro and in mouse corneas in vivo.

Using a keratin 14 expression cassette, we created transgenic mice that over-expressed podoplanin-Fc in the skin. No obvious outward phenotype was identified in these mice, but surprisingly, podoplanin-Fc—although produced specifically in the skin—entered the blood circulation and induced disseminated intravascular coagulation, characterized by microthrombi in most organs and by thrombocytopenia, occasionally leading to fatal hemorrhage. These findings re-

veal an important role of podoplanin in lymphatic vessel formation and indicate the potential of podoplanin-Fc as an inhibitor of lymphangiogenesis. These results also demonstrate the ability of podoplanin to induce platelet aggregation in vivo, which likely represents a major function of lymphatic endothelium. Finally, keratin 14 podoplanin-Fc mice represent a novel genetic animal model of disseminated intravascular coagulation. (*Blood*. 2010;116(20):4376-4384)

Introduction

Recombinant soluble fusion proteins that consist of the extracellular domain of a membrane protein linked to the Fc region of immunoglobulin G (IgG) can inhibit the function of their membrane-bound analog by sequestering its ligands and preventing them from binding to the endogenous protein. This concept is being exploited for research as well as therapeutic purposes. For example, a soluble vascular endothelial growth factor receptor (VEGFR)-3-Fc fusion protein has been used experimentally to block signaling of the VEGFR-3 ligands VEGF-C and -D and inhibit VEGF-C–induced tumor lymphangiogenesis.¹ Conversely, it is conceivable that Fc fusion proteins might mimic, and thus enhance, the effect of their respective membrane-bound analog, for example by activating ligands on the surface of other cells.

Podoplanin is a small transmembrane glycoprotein that is highly expressed on the surface of lymphatic but not blood vascular endothelial cells in vitro²⁻⁴ and in vivo.⁵⁻⁷ Despite being very short, the cytoplasmic tail of podoplanin appears to be involved in cytoskeletal organization, because it interacts with proteins of the ezrin/radixin/moesin family, which function as cross-linkers between actin filaments and the plasma membrane.⁸ The function of the podoplanin ectodomain, however, is less clear, although it comprises approximately 80% of the 162 amino acids of human podoplanin and, because of its abundant carbohydrate moieties, makes up more than 90% of the protein's molecular weight. Through its extracellular portion, podoplanin might interact with molecules on the surface of neighboring cells, with components of the extracellular matrix, or with soluble factors in the extracellular space. Three such interaction partners have been identified: the mammalian lectin galectin-8, which modulates several functions of lymphatic endothelial cells (LECs);⁹ the C-type lectin-like receptor (CLEC)-2

on the surface of platelets, which mediates podoplanin-induced platelet aggregation in vitro;^{10,11} and the lymphatic-specific chemokine (C-C motif) ligand 21 (CCL21), which is a chemoattractant for chemokine (C-C motif) receptor 7 (CCR7)–positive immune cells.¹²

Although little is known about its exact role on the lymphatic endothelium, podoplanin is required for the correct formation and function of the lymphatic vasculature.⁷ We have produced podoplanin-Fc, a fusion protein consisting of the extracellular portion of human podoplanin linked to the Fc region of human IgG₁, to inhibit or enhance the effect of endogenous, membrane-bound podoplanin and thus modulate the growth and/or function of lymphatic vessels. The induction or inhibition of lymphatic vessel growth and function is of interest for experimental and clinical applications, including the therapy of lymphedema or cancer (reviewed in Cueni and Detmar¹³).

To evaluate the potential of podoplanin-Fc as an anti- or pro-lymphangiogenic agent, we have assessed its effect in different model systems of lymphangiogenesis: in vitro, in vivo, and by ectopic expression in the skin of transgenic mice. We show that podoplanin-Fc has an inhibitory effect on lymphatic vessel formation but, unexpectedly, also potently induces platelet aggregation in transgenic mice despite restriction of transgene expression to the skin.

Methods

Production of podoplanin-Fc

Podoplanin-Fc was produced in Chinese hamster ovary (CHO) wild-type, CHO Id1D (ATCC), and human embryonic kidney (HEK) 293 cells as previously described.⁹

Submitted April 9, 2010; accepted August 5, 2010. Prepublished online as *Blood* First Edition paper, August 17, 2010; DOI 10.1182/blood-2010-04-278564.

An Inside *Blood* analysis of this article appears at the front of this issue.

The online version of this article contains a data supplement.

The publication costs of this article were defrayed in part by page charge payment. Therefore, and solely to indicate this fact, this article is hereby marked "advertisement" in accordance with 18 USC section 1734.

© 2010 by The American Society of Hematology

Immunoblot

Protein samples were boiled in Laemmli buffer, resolved in 10% polyacrylamide gels (Invitrogen), and transferred to nitrocellulose membranes (Bio-Rad Laboratories). Five percent nonfat dry milk in phosphate-buffered saline (PBS) was used for blocking and antibody dilutions. Antibodies against human podoplanin (D2-40, 1:1000; Covance Research Products; or rabbit antihuman podoplanin, 2 $\mu\text{g}/\text{mL}$; Cell Sciences) were followed by horseradish peroxidase-coupled antimouse or antirabbit antibodies (1:2000 or 1:10 000 dilutions, respectively; GE). For detection, the ECL Plus Chemiluminescent Detection System and enhanced chemiluminescence films (GE) were used.

Functional assays with human endothelial cells

Primary human dermal LECs were isolated and cultured as described.^{9,14,15} Human umbilical vein endothelial cells were obtained from ScienCell Research Laboratories and cultured the same way as the LECs. Adhesion assays were performed as described.¹⁶ Briefly, in type I collagen-coated (50 $\mu\text{g}/\text{mL}$ in PBS [Inamed Biomaterials]) 24-well cell culture plates, 6×10^4 ECs per well were incubated for 45 minutes at 37°C. Absorbance at 590 nm was measured using a VersaMax microplate reader (Molecular Devices), and the average background absorbance of empty wells was subtracted from all values. Migration assays were performed on HTS FluoroBlok Insert System 24-well plates (pore size 8 μm ; Becton Dickinson), which were coated with 50 $\mu\text{g}/\text{mL}$ type I collagen, as described.⁹ LECs (10^5 per well) were incubated for 3 hours at 37°C with podoplanin-Fc or human IgG (Sigma-Aldrich) added to both chambers of the FluoroBlok plate. Tube formation and proliferation assays were performed as described.^{9,14,15} For proliferation assays, LECs (1500 per well) were seeded; after 24 hours, fetal bovine serum concentration in the culture medium was reduced to 2%, and proteins were added 48 hours after seeding. Relative cell numbers were determined after a subsequent 48-hour incubation. For all assays, podoplanin-Fc or human IgG were added at a concentration of 0.5 μM dimeric protein, and recombinant human VEGF-A (20 ng/mL; kindly provided by the National Cancer Institute) was used as a positive control where indicated. Three (adhesion, migration, tube formation) or 8 (proliferation) replicates were performed, and the statistical significance of the data was analyzed using the unpaired Student *t* test.

Embryoid body assay

Embryoid bodies (EBs) were established in Dulbecco modified Eagle medium (DMEM) supplemented with 15% fetal bovine serum, 1mM sodium pyruvate, minimum essential medium (MEM) nonessential amino acids, 2mM L-glutamine, 100 U/mL penicillin, 100 $\mu\text{g}/\text{mL}$ streptomycin (all from Gibco) and 100nM β -mercaptoethanol (Fluka) as described.¹⁷ They were exposed to 20 ng/mL recombinant human VEGF-A, 200 ng/mL recombinant human VEGF-C (kindly provided by Dr K. Ballmer-Hofer, Paul Scherrer Institute, Villigen, Switzerland), and either 1 μM dimeric podoplanin-Fc from HEK 293 cells or 1 μM human IgG, starting 14 days after the removal of leukemia inhibitory factor (Chemicon International). The medium containing VEGF-A, VEGF-C, and podoplanin-Fc or human IgG was replaced every second day until day 22 after leukemia inhibitory factor removal. Then, EBs were fixed and stained for immunofluorescence detection of lymphatic vessel endothelial hyaluronan receptor (LYVE-1) and CD31 as described.¹⁷ Images of each EB were taken at 10 \times magnification using an Axiovert 200M inverted microscope equipped with a Plan-NEOFLUAR 10 \times /0.30 objective and an AxioCam MRm camera (Carl Zeiss). AxioVision 4.7.1 software (Zeiss) was used for image acquisition and Photoshop CS3 software (Adobe Systems) was used for image overlay. The number of individual (ie, discontinuous) CD31 positive or LYVE-1/CD31 double-positive structures was counted in each EB. Eighteen EBs were used for each condition, and the Mann-Whitney test was performed for statistical analysis of the results.

Corneal lymphangiogenesis and hemangiogenesis assay

Lymphangiogenesis was induced in the cornea of BALB/c mice by suture placement as previously described.^{18,19} All protocols were approved by the

University of California at Berkeley Animal Care and Use Committee, and animals were treated according to the Association for Research in Vision and Ophthalmology Statement for the Use of Animals in Ophthalmic and Vision Research. Mice were anesthetized using a mixture of ketamine, xylazine, and acepromazine (50, 10, and 1 mg/kg body weight, respectively) for each surgical procedure. One hundred micrograms of podoplanin-Fc from HEK 293 cells or human IgG (Sigma-Aldrich) were injected into the subconjunctival space every other day for 2 weeks after suture placement. Then, corneas were excised and lymphatic vessels visualized by immunofluorescent staining for LYVE-1 (Abcam) as described.^{18,20} The samples were observed with an Axioplan 2 epifluorescence microscope (Zeiss) and photographed with an AxioCam digital camera system (Zeiss). Lymphatic vessel growth was graded as previously described,²⁰ based on the circumferential extent of lymphatic vessels in 12 areas around the clock and the centripetal growth of the longest vascular frond in each area. In addition, corneal blood vessels were observed using a slit-lamp with an integrated digital camera system (SL-D4 and DC-3; Topcon Medical Systems) and similarly quantified. Seven to ten mice were used per group and the Mann-Whitney test was used to determine the statistical significance of the results. The double staining of Prospero homeobox protein 1 (Prox-1) and LYVE-1 was performed as described previously,²¹ using rat antimouse LYVE-1 (R&D Systems) and rabbit antimouse Prox-1 (kindly provided by Dr K. Alitalo, Helsinki, Finland) antibodies. The samples were observed and photographed with a laser-scanning confocal microscope (Zeiss 510 META NLO, AxioImager, Zeiss).

Generation of K14 podoplanin-Fc transgenic mice

The 1200-bp human podoplanin-Fc cDNA, constructed as previously described,²² was subcloned into a pBluescript KS (+) vector (Stratagene), containing a K14 expression cassette²³ (kindly provided by Dr S. Werner, ETH Zurich, Switzerland). A 4.5-kb *KpnI*-fragment (Figure 4A) was purified and used for pronuclear injection (Biomodels Austria GmbH). Transgenic lines were established on the Friend virus B-type (FVB) genetic background. For the identification of transgenic animals, genomic tail DNA was subjected to polymerase chain reaction (PCR) using the following primers: forward 5'-GAAAGCCAAGGGGAATGGAA-3' (sequence located within the K14-promotor) and reverse 5'-CAAGCCAGACTTAT-AGCGGTCTTC-3' (sequence located within the podoplanin gene). For detection of podoplaninFc mRNA, total RNA was reverse transcribed using the High Capacity cDNA Reverse Transcription Kit (Applied Biosystems). Primers specific for human podoplanin (5'-AGGCGGCGTTGCCAT-3', 5'-GTCTTCGCTGGTCTCTGGAG-3'), or mouse β -actin (pre-designed QT01136772; QIAGEN), or the genotyping primers were used.

Blood and tissue sampling

Blood was collected from deeply anesthetized animals (120 mg/kg ketamine, 0.3 mg/kg medetomidine) by cardiac puncture and submitted to hematological analysis at the Clinical Laboratory, Vetsuisse Faculty, University of Zurich, Switzerland. Tissues collected for immunohistochemical analyses were fixed in 4% paraformaldehyde overnight at 4°C, immersed in 30% sucrose for 24 to 48 hours at 4°C, embedded in optimal cutting temperature compound (Sakura) and frozen at -80°C . For immunoblot analyses, tissue samples were homogenized in lysis buffer (20mM Tris [tris(hydroxymethyl)aminomethane] pH 7.4, 150mM NaCl, 5mM EDTA [ethylenediaminetetraacetic acid], 1% Triton X-100, 25mM sodium fluoride, 1mM phenylmethanesulfonyl fluoride, 1mM sodium metavanadate, 10% glycerol and protease inhibitor cocktail [Roche Diagnostics]), and protein was extracted for 30 minutes on ice. Total RNA was isolated from RNeasy (Ambion)-stabilized tissue samples using the RNeasy Mini kit (QIAGEN). On-column DNase digestion was performed according to the manufacturer's instructions.

Immunohistochemistry

Immunohistochemistry was performed on 7- μm cryostat sections using an antibody against human podoplanin (2 $\mu\text{g}/\text{mL}$; Cell Sciences), followed by

biotinylated antirabbit secondary antibody (5 µg/mL; Vector). The Vectastain ABC and the AEC (3-amino-9-ethylcarbazole) substrate kits (Vector) were used for chromogenic detection, and nuclei were counterstained with hematoxylin. Images were taken with an Axioskop 2 microscope equipped with Plan-APOCHROMAT 10×/0.45 and Plan-NEOFLUAR 40×/0.75 objectives and an AxioCam MRc camera (Zeiss). AxioVision 4.7.1 software was used for image acquisition.

Flow cytometry

Detection of podoplanin-Fc binding to platelets and platelet activation by flow cytometry was performed essentially as described,²⁴ using recombinant human podoplanin-Fc or VEGFR-3-Fc as negative control (both from R&D Systems). Platelet-rich plasma (PRP) from wild-type FVB mice was used in these experiments, obtained by dilution (1:3) of heparinized blood in Tyrodes buffer (137mM NaCl, 2.7mM KCl, 0.2mM Na₂HPO₄, 12mM NaHCO₃, 5.5mM D-glucose, 1mM MgCl₂, 1mM CaCl₂), centrifugation at 100 × g for 15 minutes, and collection of the upper phase as PRP.

In vitro blood coagulation experiments

Blood was collected by cardiac puncture from wild-type FVB mice and diluted 10:1 with acid-citrate dextrose (ACD) anticoagulant (20mM citric acid, 110mM sodium citrate, 5mM dextrose). Michigan Cancer Foundation-7 (MCF7) human breast carcinoma cells, overexpressing or not human podoplanin, were detached from culture plates by repeated PBS rinses, and approximately 5 × 10⁴ cells in 5 µL of PBS were added to 44 µL of blood samples. Coagulation was initiated by addition of 1 µL of 500mM calcium chloride, and samples were mixed by gentle vortexing. After exactly 1 minute incubation time, tubes were inverted and the extent of coagulation was determined visually.

Results

Podoplanin-Fc inhibits adhesion, migration and tube formation of LECs

We produced 3 glycoforms of podoplanin-Fc, a soluble Fc fusion protein comprising the ectodomain of human podoplanin, in mammalian cell lines differing in their glycosylation capacity. HEK 293 cells, which assemble extended, branched O-linked oligosaccharides, were used to make extensively glycosylated podoplanin-Fc. A protein with only short O-glycans of the core 1 structure was made in CHO wild-type cells,^{25,26} and an unglycosylated form was made in CHO ldlD cells, which are unable to produce any O-linked carbohydrate chains when cultured in a medium with glucose as the sole sugar source.²⁷ The correct glycosylation, the purity, and the dimeric conformation of podoplanin-Fc proteins were verified by immunoblot, silver staining, and gel filtration, respectively (supplemental Figure 1, available on the *Blood* Web site; see the Supplemental Materials link at the top of the online article), and bacterial endotoxins were removed if required.

To determine whether soluble podoplanin-Fc affects the function of endogenous podoplanin, we added it to cultured primary human LECs and assessed several cellular functions, including proliferation, adhesion, migration, and the formation of tube-like structures, by standard assays established in our laboratory.^{9,14,15} Human IgG served as the control to account for potential effects of the Fc part of the fusion protein. Compared with controls, podoplanin-Fc slightly inhibited LEC adhesion to type I collagen (up to -21%, $P = .0049$; Figure 1A) and haptotactic migration toward type I-collagen (up to -34%, $P = .0046$; Figure 1B). Furthermore, exposure to podoplanin-Fc reduced the formation of tube-like structures by LECs in type I collagen gels by up to 73% ($P = .013$; Figure 1C). Interestingly, the less glycosylated proteins

produced in CHO wild-type or CHO ldlD cells were more effective than the more extensively glycosylated protein produced in HEK 293 cells. Podoplanin-Fc did not have a general cytotoxic effect because podoplanin-Fc from CHO wild-type cells, which was the most effective inhibitor of LEC adhesion, migration, and tube formation, did not affect the proliferation of LECs (Figure 1D). Importantly, podoplanin-Fc did not affect cellular functions of human umbilical vein endothelial cells (supplemental Figure 2).

Podoplanin-Fc inhibits lymphatic vessel formation in mouse EBs in vitro

We next investigated whether podoplanin-Fc might also inhibit lymphatic vessel growth in more complex models of lymphangiogenesis. Mouse EBs are 3-dimensional, embryonic stem cell-derived structures in which the formation of lymphatic vessel-like structures can be induced by lymphangiogenic growth factors.¹⁷ We used a combination of VEGF-A and VEGF-C to promote lymphatic vessel formation in EBs. Simultaneously, EBs were exposed to podoplanin-Fc (from HEK 293 cells) or human IgG for 8 days, starting at day 14 after EB formation when lymphatic vessel-like structures, coexpressing the lymphatic marker LYVE-1 and the pan-endothelial marker CD31, first appear in the EBs (D.M., unpublished observation), although only a minority of these structures also express Prox-1. In agreement with the ability of podoplanin-Fc to inhibit several LEC functions, it also reduced the formation of LYVE-1/CD31 double-positive lymphatic vessel-like structures in EBs, compared with human control IgG (Figure 2A). Quantification revealed a 55% reduction in the median number of lymphatic vessel-like structures per EB after podoplanin-Fc treatment, compared with control ($P = .013$, $n = 18$; Figure 2B), whereas the median number of CD31 positive/LYVE-1 negative blood vessel-like structures was not significantly changed (Figure 2C).

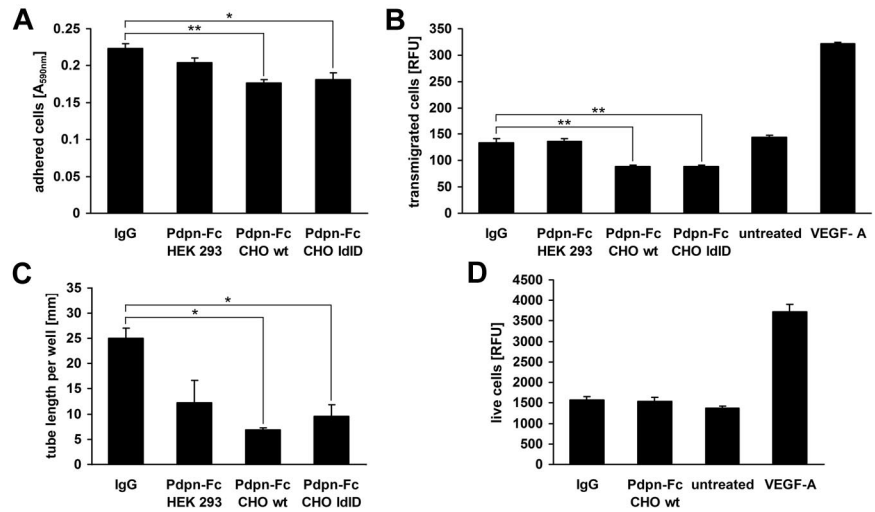
Podoplanin-Fc impairs lymphatic vessel formation in inflamed mouse corneas in vivo

Next, we assessed the effects of podoplanin-Fc in a well-established in vivo model of lymphangiogenesis: suture-induced inflammatory neovascularization of the mouse cornea.^{18,19,28} The brief inflammatory insult inflicted on the normally avascular cornea by suture placement induces the growth of blood and lymphatic vessels. Mice were given repeated subconjunctival injections of podoplanin-Fc or control IgG for 2 weeks after suture placement. Treatment with podoplanin-Fc significantly suppressed corneal lymphangiogenesis based on the circumferential extent and centripetal growth of LYVE-1 positive lymphatic vessels (-26%, $P < .05$, $n_{\text{IgG}} = 10$, $n_{\text{Pdpn-Fc}} = 7$; Figure 3A-B), although no significant difference was detected on blood vessel scores between the treatment and control groups (supplemental Figure 3A). Double staining for LYVE-1 and Prox-1 revealed that the LYVE-1-positive vessels in the inflamed cornea coexpressed Prox-1, further confirming their lymphatic origin (Figure 3C). Interestingly, in the corneas exposed to podoplanin-Fc, some potentially embolized blood vessels were observed (supplemental Figure 3B), indicating that podoplanin-Fc treatment might promote blood coagulation.

Targeted overexpression of podoplanin-Fc in the skin of transgenic mice

To more closely assess the effect of podoplanin-Fc in vivo, we established transgenic mice that overexpressed podoplanin-Fc

Figure 1. Podoplanin-Fc inhibits functions of LECs in vitro. (A) Primary human LECs were allowed to adhere to type I collagen-coated cell culture plates for 45 minutes in the presence of 0.5 μ M podoplanin-Fc glycoforms or human IgG. Attached cells were stained with crystal violet and the absorbance of subsequently resolubilized dye was measured at 590 nm. (B) Haptotactic migration of LECs toward type I collagen was assessed in a 2-chamber assay for 3 hours in the presence of 0.5 μ M podoplanin-Fc glycoforms or human IgG. Chemotactic migration toward 20 ng/mL VEGF-A served as positive control. Transmigrated cells were stained with calcein and fluorescence intensity (RFU) at λ_{ex} 485 nm/ λ_{em} 539 nm was measured. (C) Tube formation by LECs was assessed in type I collagen gels containing 0.5 μ M podoplanin-Fc glycoforms or human IgG. The length of tube-like structures was determined after 14 hours in three 5 \times magnified images per well. (D) Proliferation of LECs was assessed in the presence of 0.5 μ M podoplanin-Fc from CHO wild-type cells or human IgG, or 20 ng/mL VEGF-A. Live cells were stained after 48 hours with 4-methylumbelliferyl heptanoate and fluorescence intensity (RFU) at λ_{ex} 355 nm/ λ_{em} 450 nm was measured. Data represent mean \pm standard error of the mean (n = 3 [A-C] or n = 8 [D]), ** P < .01, * P < .05.



specifically in the skin using a K14 promoter cassette (Figure 4A). No obvious phenotypic differences were observed between the 5 transgenic founder lines that were established or between transgenic and wild-type animals. Transgenic animals were fertile and outwardly appeared healthy. No gross morphological abnormalities were found in the skin or any other organs by histological examination at 6 to 8 weeks of age (not shown). Transgene expression was confirmed by detection of podoplanin-Fc mRNA and protein by reverse transcription (RT) PCR and immunoblot analyses, respectively, in the skin of 6-week-old transgenic but not wild-type mice (Figure 4B,D). Podoplanin-Fc mRNA was not detectable in any organs other than the skin (Figure 4C), demonstrating the restriction of transgene expression to the skin. Accordingly, podoplanin-Fc protein was not detectable in tissue lysates of intestines. Surprisingly, however, small amounts of podoplanin-Fc protein were found in lysates of livers from transgenic mice (Figure 4D). Immunohistochemical staining for human podoplanin in dorsal skin sections from transgenic mice confirmed strong expression of the transgene in basal epidermal keratinocytes and in the outer root sheath keratinocytes of hair follicles, the expected sites of K14 promoter activity²³ (Figure 4E). In addition, diffuse staining was observed in the other parts of the skin, suggesting that the protein diffuses within the tissue, away from its place of secretion

(Figure 4E). In contrast, wild-type littermate controls were negative for human podoplanin mRNA and protein (Figure 4B,D-E).

Podoplanin-Fc induces disseminated intravascular coagulation (DIC) in K14 podoplanin-Fc transgenic mice

Although K14 podoplanin-Fc transgenic mice were outwardly indistinguishable from their wild-type littermates, in the founder line with the highest level of transgene expression, 15% of the animals died between the ages of 3 and 6 weeks. The majority (75%) of the animals that died were male. The mice died suddenly, without previous signs of deteriorated condition. Death appeared to be provoked by intense activity or exposure to stress, as occasionally occurred when mice were handled. Because podoplanin-Fc expression was restricted to the skin, its lethal effect was surprising. We investigated whether podoplanin-Fc could be detected in the systemic circulation and/or other organs than the skin. Its presence in parts of the skin that lack K14 promoter activity (Figure 4E) indicates that the protein diffused. Indeed, podoplanin-Fc was detected by immunoblot analysis in the serum of transgenic but not wild-type mice (Figure 5A). Based on enzyme-linked immunosorbent assay quantification, serum concentrations of podoplanin-Fc in transgenic animals were estimated to be greater than 10nM (not

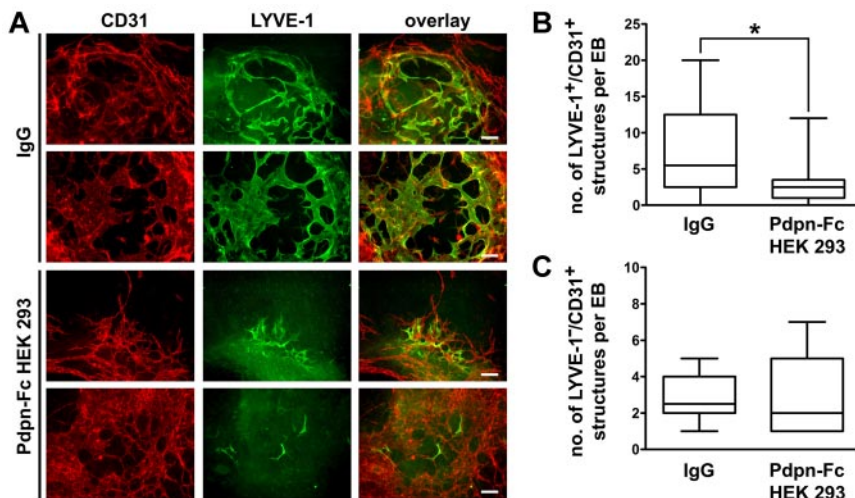


Figure 2. Podoplanin-Fc inhibits lymphatic vessel formation in mouse EBs in vitro. (A) Lymphatic and blood vessel-like structures were visualized by immunofluorescent staining for the lymphatic marker LYVE-1 (green) and the pan-endothelial marker CD31 (red), in mouse EBs exposed to human VEGF-A (20 ng/mL), human VEGF-C (200 ng/mL), and podoplanin-Fc or human IgG (1 μ M) from days 14 to 22 after EB formation. Bars represent 100 μ m. (B) LYVE-1 and CD31 double-positive lymphatic vessel-like structures and (C) CD31 positive blood vessel-like structures per EB were quantified. The number of individual structures is depicted as a boxplot, representing the median, minimum, and maximum data values and upper and lower quartiles. * P = .013 (n = 18).

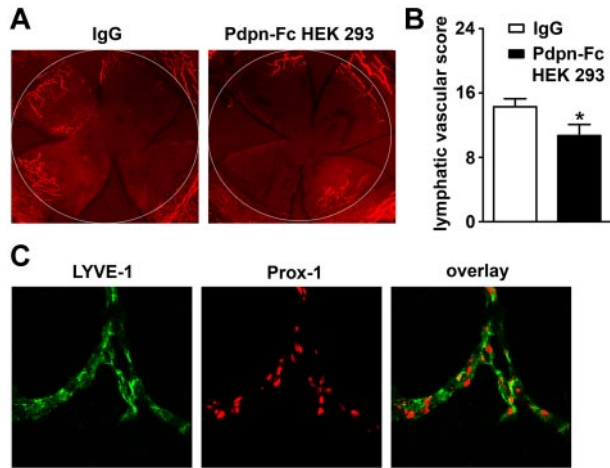


Figure 3. Podoplanin-Fc suppresses lymphangiogenesis in inflamed mouse corneas in vivo. (A) Representative whole-mount micrographs of corneal lymphatic vessels, visualized by immunofluorescent staining for the lymphatic marker LYVE-1 (red) after 2 weeks of treatment with human IgG or podoplanin-Fc (100 μ g, injected every second day into subconjunctival space). Original magnification $\times 25$. White circle: demarcation between the cornea and conjunctiva. (B) Summary of lymphatic vascular scores, determined for each cornea based on the circumferential extent and centripetal growth of lymphatic vessels. Data represent mean \pm standard error of the mean ($n_{\text{IgG}} = 10$, $n_{\text{Pdpn-Fc}} = 7$), * $P < .05$. (C) Representative micrographs of corneal lymphatic vessels double-stained for LYVE-1 (green) and Prox-1 (red). Original magnification $\times 400$.

shown). Moreover, immunohistochemical analysis of tissue sections from lung, heart, intestine, liver and kidney of transgenic mice proved the presence of podoplanin-Fc in and around blood vessels of tissues other than the skin (Figure 5B). These results revealed that, although podoplanin-Fc was produced locally in the skin, it was distributed throughout the bodies of transgenic animals via the blood circulation.

We next sought to identify the cause of the sudden death of the transgenic mice. Careful necropsy of a moribund transgenic

mouse revealed acute intestinal hemorrhage. The small intestine of the animal appeared to be filled with blood, whereas the liver, mucous membranes, and serosal surfaces were very pale and anemic compared with those of a wild-type littermate (Figure 6A). In agreement with this finding, melena (dark, hemoglobin stained feces) was observed during postmortem examinations of several transgenic animals. In addition, dead animals occasionally displayed signs of epistaxis (ie, bleeding at the snout). Nevertheless, causes of death other than bleeding cannot be ruled out in animals with extensive postmortem changes compromising pathological analysis.

Histological examination of surviving, seemingly healthy animals revealed conspicuous, podoplanin-positive thrombi in blood vessels in the lamina propria of the intestinal mucosa of transgenic mice that were not observed in wild-type mice (Figure 6B). Similar thrombi were also found in other organs, including the heart, lung, liver, kidney, and—importantly—the brain of transgenic mice (Figure 6C), even before animals showed any signs of morbidity. We assessed the time needed for blood coagulation in 8-week-old transgenic and wild-type mice by clipping off a piece of the tail tip from anesthetized animals and measuring the time until the cessation of bleeding. In wild-type animals, bleeding stopped 7 to 15 minutes after wounding, whereas K14 podoplanin-Fc transgenic mice continued to bleed heavily for 60 minutes, at which time they were euthanized (Figure 6D). In agreement with the observed impaired coagulation, hematological analysis revealed significant thrombocytopenia in transgenic mice compared with wild-type littermates (350×10^3 versus 980×10^3 thrombocytes per μL of blood, respectively; Figure 6E). However, there were no differences in any other parameters such as hematocrit and hemoglobin concentrations, or erythrocyte, leukocyte, and reticulocyte counts (not shown). Together, these results suggest that K14 podoplanin-Fc mice suffer from DIC, a consumption coagulopathy leading to bleeding diathesis caused by depletion of thrombocytes.

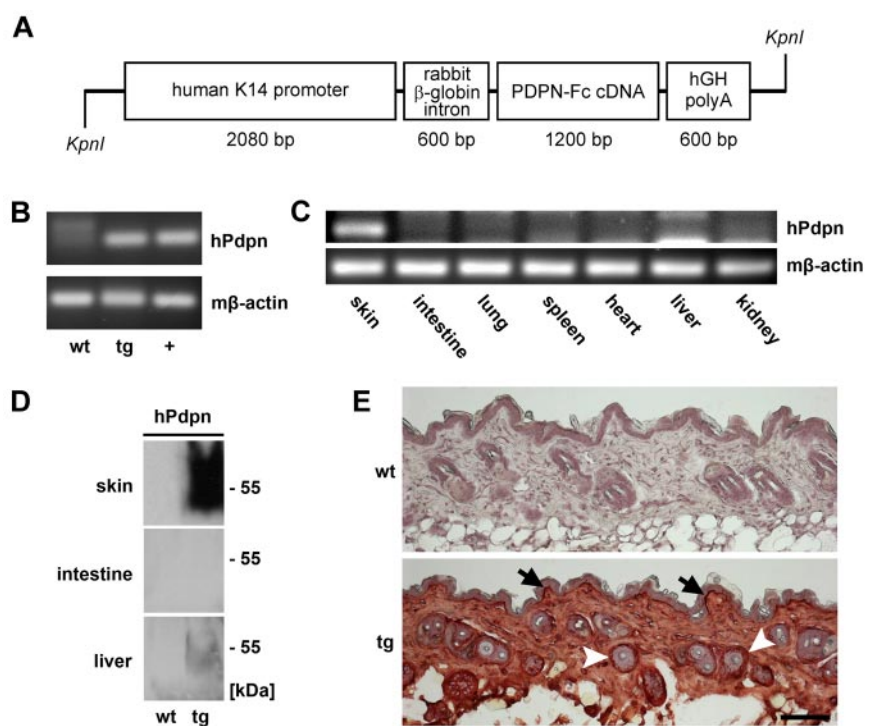
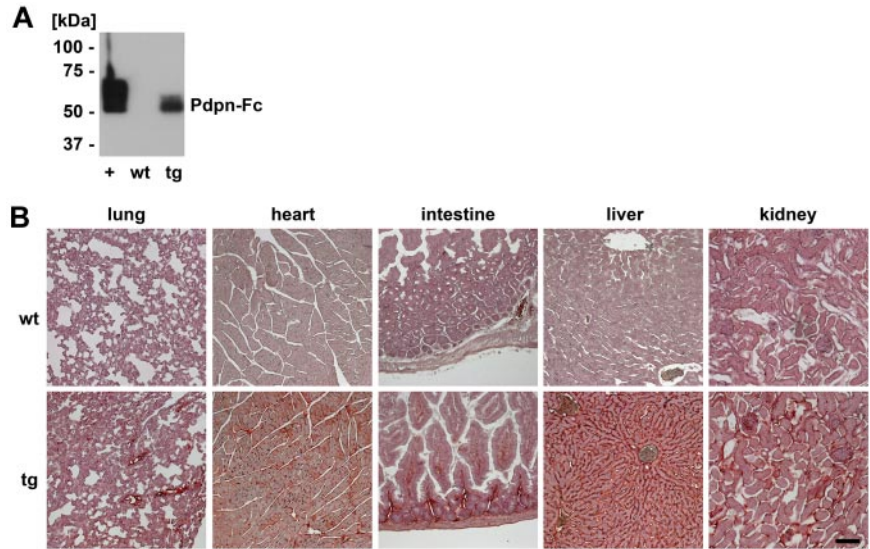


Figure 4. Targeted overexpression of podoplanin-Fc in the skin of transgenic mice. (A) Schematic representation of the K14 podoplanin-Fc transgene construct. (B) Human podoplanin mRNA was detected by RT-PCR using total RNA (200 ng) extracted from the skin of wild-type and K14 podoplanin-Fc transgenic mice. RNA (100 ng) from mouse cells transfected with human podoplanin cDNA was used as positive control (+). (C) Human podoplanin mRNA was detected by RT-PCR using total RNA (300 ng) extracted from different organs of K14 podoplanin-Fc transgenic mice. (D) Podoplanin-Fc (50-55 kDa) was detected by immunoblot analysis of tissue lysates from skin, intestine, and liver of wild-type and transgenic mice. (E) Podoplanin-Fc was detected by immunohistochemical analysis of paraformaldehyde-fixed cryosections of dorsal skin samples taken from wild-type and transgenic mice at 6 weeks of age. It was expressed at high levels in the basal keratinocyte layer (arrows) and in the outer root sheath keratinocytes of hair follicles (arrowheads). Bar represents 100 μm . Immunoblot and immunohistochemical analyses were performed using antibodies directed against human podoplanin. *wt* wild-type; *tg* transgenic; *hPdpn* human podoplanin.

Figure 5. Podoplanin-Fc is present in the blood circulation of K14 podoplanin-Fc transgenic mice. (A) Podoplanin-Fc was detected by immunoblot analysis of serum samples (4 μ L) from K14 podoplanin-Fc transgenic and wild-type mice for human podoplanin. Podoplanin-Fc from HEK 293 cells (approximately 1 pmol) was used as positive control (+). (B) Podoplanin-Fc was detected by immunohistochemical analysis of different organs of transgenic and wild-type mice. Bar represents 100 μ m. *wt* wild-type; *tg* transgenic.



Podoplanin binds to platelets and induces platelet activation and blood coagulation in vitro

Several experiments were performed to rule out the possibility that podoplanin-Fc induces platelet aggregation via its Fc portion. As determined by flow cytometry, human podoplanin-Fc, but not human VEGFR-3-Fc, bound to CD41-positive platelets (Figure 7A-B). Moreover, fibrinogen binding to platelets was enhanced in the presence of podoplanin-Fc but not VEGFR-3-Fc (Figure 7C), demonstrating that podoplanin-Fc, but not another Fc fusion protein, can bind and activate platelets. To further confirm that podoplanin is able to induce blood coagulation independently of the Fc portion of the fusion protein, we assessed the capacity of

podoplanin-overexpressing cells to coagulate mouse blood. Indeed, MCF7 human breast carcinoma cells expressing (transmembrane) human podoplanin on their surface accelerated coagulation of mouse blood, compared with MCF7 control cells, after overriding citrate-anticoagulation by an excess of calcium chloride (Figure 7D).

Discussion

We found that a recombinant soluble protein in which Fc was fused to the extracellular domain of podoplanin reduced adhesion, haptotactic

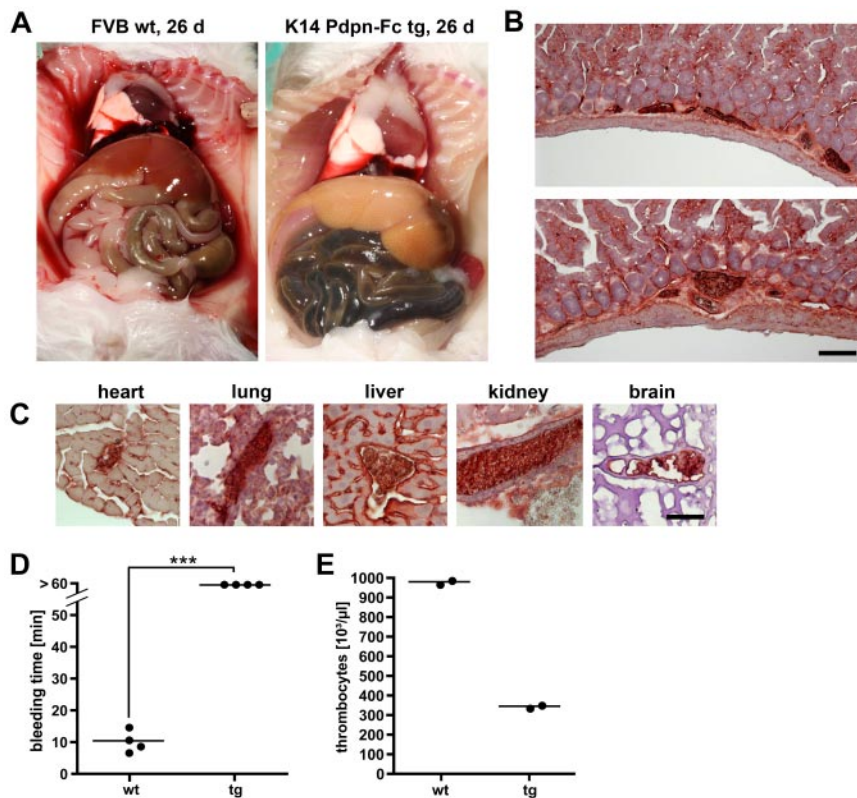


Figure 6. Podoplanin-Fc induces disseminated intravascular coagulation, leading to thrombocyte consumption and bleeding diathesis. (A) A transgenic mouse was examined postmortem after spontaneous death and compared with a wild-type littermate at an age of 26 days. Melena, pale liver, and serosa suggest bleeding to the intestine. (B-C) Embolized blood vessels were observed on cryosections of intestine (B) and other organs (C) of transgenic mice, immunohistochemically stained for human podoplanin. (D) Times until the cessation of bleeding after tail clipping of wild-type and transgenic mice were measured. *** $P < .001$. (E) Thrombocyte counts in the blood of wild-type and transgenic mice were determined. Bars represent 100 μ m (B) and 25 μ m (C). *wt* wild-type; *tg* transgenic.

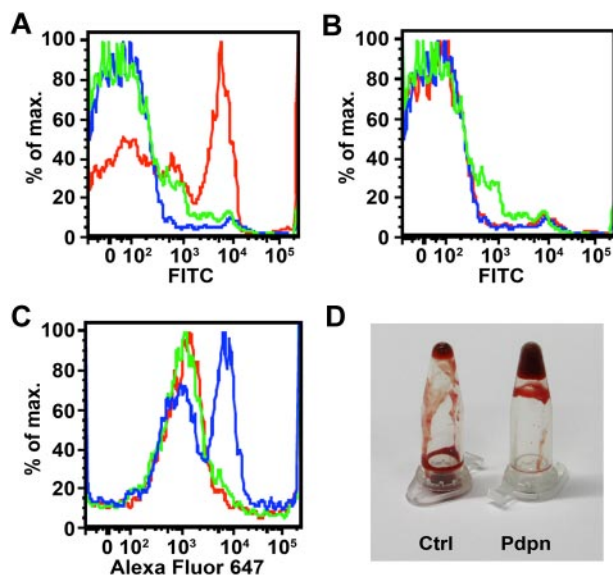


Figure 7. Podoplanin binds to platelets and induces platelet activation and blood coagulation in vitro. (A–B) Mouse PRP was incubated with human podoplanin-Fc (A) or VEGFR-3-Fc (B), and Fc fusion proteins bound to CD41⁺ platelets were subsequently detected by flow cytometry, using a rabbit antihuman IgG Fc γ antibody followed by fluorescein isothiocyanate (FITC)-conjugated antirabbit antibody (red) or isotype control antibody (green). Blue: incubation without Fc fusion protein. (C) Mouse PRP was incubated with human podoplanin-Fc or VEGFR-3-Fc, before Alexa Fluor 647-conjugated human fibrinogen was added. Fibrinogen bound to CD41⁺ platelets was subsequently detected by flow cytometry. Blue: incubation with podoplanin-Fc; green: incubation with VEGFR-3-Fc; red: incubation without Fc fusion protein. (D) MCF7 cells overexpressing human podoplanin (Pdpn) or control MCF7 cells (Ctrl) were added to samples of citrate-anticoagulated mouse blood. One minute after initiation of coagulation by addition of calcium chloride, tubes were inverted and the fluidity of the blood observed.

migration, and tube formation of cultured primary human LECs but not of blood vascular ECs. Importantly, podoplanin-Fc also inhibited lymphatic but not blood vessel formation in mouse EBs and suppressed lymphogenesis but not hemangiogenesis in mouse corneas. Together, these results indicate that podoplanin-Fc interferes with the function of endogenous, membrane-bound podoplanin on the surface of LECs. It is conceivable that podoplanin-Fc sequesters soluble ligands of podoplanin or occupies binding sites for podoplanin in the extracellular matrix and/or on neighboring cells. The fact that podoplanin-Fc inhibited several functions of cultured LECs in vitro suggests the presence of a ligand for podoplanin-Fc on the cells themselves—perhaps adhesion molecules such as integrins, which are essential for all of the tested cellular functions. Alternatively, because all functional assays were performed in the presence of collagen (which was previously found to be a suitable substrate for the assessment of LEC functions), podoplanin-Fc might interact with and interfere with the binding of LECs to this extracellular matrix molecule. However, we did not detect an interaction between podoplanin-Fc and collagen itself by either enzyme-linked immunosorbent assay or coimmunoprecipitation experiments (not shown).

Remarkably, despite the facts that human and mouse podoplanin have only 48% amino acid sequence identity and that the ectodomain is the least-conserved portion of the protein,²⁹ podoplanin-Fc, which contains the extracellular domain of human podoplanin, impaired lymphangiogenesis in mouse EBs and corneas. Its interaction with the relevant ligands must therefore be mediated by a part of the podoplanin ectodomain that is conserved between human and mouse. There are no obvious conserved peptide motifs that immediately would impose themselves as candidate mediators

of these interactions. However, because human and mouse podoplanin are both heavily glycosylated,^{29,30} interactions with other proteins could also depend on the carbohydrate moieties present in their ectodomains. This is the case for the interactions between human podoplanin and the chemokine (C-C motif) ligand 21,¹² the platelet activation receptor CLEC-2,^{11,26} or the mammalian lectin galectin-8.⁹ To assess the relevance of its glycosylation, we compared the effects of different glycoforms of podoplanin-Fc. The protein produced in CHO wild-type cells (the glycosylation pattern of which most closely resembles the one of the endogenous protein²⁹) and the unglycosylated CHO IdD-derived protein were more effective in inhibiting the functions of human LECs in vitro than the extensively glycosylated form of podoplanin-Fc produced by HEK 293 cells. This finding suggests that interactions with podoplanin ligands on the surface of LECs do not necessarily depend on podoplanin glycosylation or that these interactions are even hindered by extensive carbohydrate structures in the podoplanin ectodomain. Nevertheless, the glycosylated HEK 293-derived podoplanin-Fc (the only glycoform that could be produced in sufficient quantity for these experiments) inhibited the formation of lymphatic vessels in mouse EBs and cornea. Thus, in more complex biological systems, additional, glycosylation-dependent podoplanin-binding partners seem to exist—for instance cytokines or extracellular matrix components—which substantially contribute to the inhibition of lymphangiogenesis by podoplanin-Fc. Moreover, the carbohydrate structures might protect the protein from protease activity and enhance its biological activity through prolonging its half-life.

It was reported that podoplanin can aggregate platelets in vitro,³¹ and we observed potentially embolized blood vessels in the corneas of mice after subconjunctival injections of podoplanin-Fc. Thus, given the potential of podoplanin-Fc to serve as an anti-lymphangiogenic agent for therapeutic purposes, we wanted to assess whether the protein would cause any unfavorable side effects in vivo, even when administered locally. Transgenic mice that overexpressed podoplanin-Fc specifically in the epidermis showed no obvious outward phenotype. However, even though podoplanin-Fc was produced locally in the skin, it readily diffused into the blood, where it induced DIC that caused thrombocytopenia and severe bleeding diathesis. Although the condition was lethal only to relatively few mice during the observation period of up to 9 months, it is of note that the signs of DIC (namely, thrombi throughout the circulation, defective blood clotting, and thrombocytopenia) were detected in all transgenic animals that were examined, despite their healthy outwardly appearance.

It is known that activation of platelets can be mediated through Fc γ receptors on their surface. The finding that podoplanin-Fc, but not VEGFR-3-Fc, was able to bind and activate platelets, and that cells expressing transmembrane podoplanin promoted the coagulation of blood samples demonstrates, however, that podoplanin is able to induce platelet activation and blood clotting independently of the Fc portion of the fusion protein. Moreover, in numerous transgenic mouse models the presence of Fc fusion proteins in the blood circulation was never reported to cause any coagulation phenotype, although identical Fc domains of the human IgG₁ subclass were involved and serum concentrations were in a similar range as in K14 podoplanin-Fc mice.^{32–39} In particular, in K14 VEGFR-3-Fc mice³⁵ we could not detect any signs of DIC, further supporting the notion that the extracellular domain of podoplanin rather than the Fc portion of the fusion protein caused platelet aggregation in K14 podoplanin-Fc mice.

This study provides the first direct *in vivo* demonstration of the potent platelet aggregation activity of podoplanin, an activity that could be relevant to lymphatic vascular function in that abnormal anastomoses between lymphatic and blood vessels may be sealed by formation of thrombi at sites of contact of platelets with podoplanin on lymphatic endothelium. This hypothesis is supported by the recent identification of the receptor for podoplanin on the surface of platelets—CLEC-2,¹⁰ which signals via the tyrosine kinase Syk and the adaptor protein SLP-76.⁴⁰ Interestingly, Syk/SLP-76 knockout mice display abnormal connections between blood and lymphatic vessels.⁴¹ A similar phenotype, featuring blood-filled lymphatic vessels, has recently also been reported for podoplanin knockout mice and mice with an endothelial cell-specific deletion of the glycosyltransferase T-synthase, which results in reduced podoplanin expression.⁴² These phenotypes indicate that LEC-expressed podoplanin prevents blood vascular-lymphatic connections.

K14 podoplanin-Fc transgenic mice might serve as a novel genetic animal model for the study of DIC, a severe complication associated with a wide variety of human diseases such as sepsis, trauma, and cancer (reviewed by Levi and Ten Cate⁴³). Inasmuch as the CLEC-2 receptor, which mediates podoplanin-induced platelet aggregation, is also activated by the snake venom rhodocytin,⁴⁰ it is worth noting that DIC also develops as a consequence of snake envenomation.⁴³ The pathological findings in K14 podoplanin-Fc mice closely resemble the human condition, which is characterized by the development of microthrombi throughout the circulation, consumption of platelets, and perturbed blood coagulation, and clinically manifests with bleeding at various sites, including the gastrointestinal tract and the nasal and gingival mucosa.⁴³ Interestingly, although animals of both sexes suffered from DIC, the mortality of male K14 podoplanin-Fc transgenic mice was greater than that of female mice. The observation that the disorder is more severe in male mice is in agreement with male sex being a risk factor for thrombotic diseases in humans.⁴⁴⁻⁴⁷

Collectively, our findings reveal an important role for podoplanin in lymphatic vessel formation and function *in vitro* and *in vivo*. They also reveal podoplanin-Fc as a potential antilymphangiogenic agent, which might be used to inhibit lymphatic

vessel growth and/or function, for instance in cancer therapy. The phenotype of K14 podoplanin-Fc transgenic mice impressively demonstrates the potent platelet aggregation activity of podoplanin *in vivo*, which is likely of relevance to lymphatic vascular function but would have to be eliminated (eg, by mutation of the crucial threonine-52³¹) to enable the development of podoplanin-Fc as a therapeutic.

Acknowledgments

We thank Dr. S. Werner for providing the K14 expression vector and for helpful discussions, Dr. K. Ballmer-Hofer for recombinant human VEGF-C, Dr. K. Alitalo for the antiProx-1 antibody, Dr. D. Kerjaschki and Dr. L. Asmis for helpful discussions, Carlos Ochoa for animal caretaking, Martin Schulz for help with EBs, Jeanette Scholl for help with histology, and Cornelius Fischer for photographs of mice.

This work was supported by National Institutes of Health grant CA69184; Swiss National Science Foundation grant 3100A0-108207; Austrian Science Foundation grant S9408-B11; Cancer League Zurich, Oncosuisse and Commission of the European Communities grant LSHC-CT-2005-518178 (M.D.); National Institutes of Health grant EY17392; and Junior Faculty Research grant from University of California at Berkeley (L.C.).

Authorship

Contribution: L.N.C. designed the research, performed experiments, analyzed results, made the figures, and wrote the paper; L.C., H.Z., D.M., R.H., A.A., and R.B. performed experiments, analyzed results, and wrote the paper; and M.D. designed the research, analyzed results and wrote the paper.

Conflict-of-interest disclosure: The authors declare no competing financial interests.

Correspondence: Michael Detmar, Institute of Pharmaceutical Sciences, Swiss Federal Institute of Technology, ETH Zurich, Wolfgang Pauli-Str 10, HCI H303, CH-8093 Zurich, Switzerland; e-mail: michael.detmar@pharma.ethz.ch.

References

- Karpanen T, Egeblad M, Karkkainen MJ, et al. Vascular endothelial growth factor C promotes tumor lymphangiogenesis and intralymphatic tumor growth. *Cancer Res*. 2001;61(5):1786-1790.
- Kriehuber E, Breiteneder-Geleff S, Groeger M, et al. Isolation and characterization of dermal lymphatic and blood endothelial cells reveal stable and functionally specialized cell lineages. *J Exp Med*. 2001;194(6):797-808.
- Petrova TV, Makinen T, Makela TP, et al. Lymphatic endothelial reprogramming of vascular endothelial cells by the Prox-1 homeobox transcription factor. *EMBO J*. 2002;21(17):4593-4599.
- Hirakawa S, Hong YK, Harvey N, et al. Identification of vascular lineage-specific genes by transcriptional profiling of isolated blood vascular and lymphatic endothelial cells. *Am J Pathol*. 2003;162(2):575-586.
- Wetterwald A, Hoffstetter W, Cecchini MG, et al. Characterization and cloning of the E11 antigen, a marker expressed by rat osteoblasts and osteocytes. *Bone*. 1996;18(2):125-132.
- Breiteneder-Geleff S, Soleiman A, Kowalski H, et al. Angiosarcomas express mixed endothelial phenotypes of blood and lymphatic capillaries: podoplanin as a specific marker for lymphatic endothelium. *Am J Pathol*. 1999;154(2):385-394.
- Schacht V, Ramirez MI, Hong YK, et al. T1alpha/podoplanin deficiency disrupts normal lymphatic vasculature formation and causes lymphedema. *EMBO J*. 2003;22(14):3546-3556.
- Martin-Villar E, Megias D, Castel S, Yurrita MM, Vilaro S, Quintanilla M. Podoplanin binds ERM proteins to activate RhoA and promote epithelial-mesenchymal transition. *J Cell Sci*. 2006;119(Pt 21):4541-4553.
- Cueni LN, Detmar M. Galectin-8 interacts with podoplanin and modulates lymphatic endothelial cell functions. *Exp Cell Res*. 2009;135:1715-1723.
- Suzuki-Inoue K, Kato Y, Inoue O, et al. Involvement of the snake toxin receptor CLEC-2, in podoplanin-mediated platelet activation, by cancer cells. *J Biol Chem*. 2007;282(36):25993-26001.
- Kato Y, Kaneko MK, Kunita A, et al. Molecular analysis of the pathophysiological binding of the platelet aggregation-inducing factor podoplanin to the C-type lectin-like receptor CLEC-2. *Cancer Sci*. 2008;99(1):54-61.
- Kerjaschki D, Regele HM, Moosberger I, et al. Lymphatic neoangiogenesis in human kidney transplants is associated with immunologically active lymphocytic infiltrates. *J Am Soc Nephrol*. 2004;15(3):603-612.
- Cueni LN, Detmar M. The lymphatic system in health and disease. *Lymphat Res Biol*. 2008;6(3-4):109-122.
- Banziger-Tobler NE, Halin C, Kajjya K, Detmar M. Growth hormone promotes lymphangiogenesis. *Am J Pathol*. 2008;173(2):586-597.
- Shin JW, Huggenberger R, Detmar M. Transcriptional profiling of VEGF-A and VEGF-C target genes in lymphatic endothelium reveals endothelial-specific molecule-1 as a novel mediator of lymphangiogenesis. *Blood*. 2008;112(6):2318-2326.
- Streit M, Velasco P, Brown LF, et al. Overexpression of thrombospondin-1 decreases angiogenesis and inhibits the growth of human cutaneous squamous cell carcinomas. *Am J Pathol*. 1999;155(2):441-452.
- Liersch R, Nay F, Lu L, Detmar M. Induction of lymphatic endothelial cell differentiation in embryoid bodies. *Blood*. 2006;107(3):1214-1216.
- Chen L, Hamrah P, Cursiefen C, et al. Vascular endothelial growth factor receptor-3 mediates

- induction of corneal alloimmunity. *Nat Med*. 2004; 10(8):813-815.
19. Chen L, Cursiefen C, Barabino S, Zhang Q, Dana MR. Novel expression and characterization of lymphatic vessel endothelial hyaluronate receptor 1 (LYVE-1) by conjunctival cells. *Invest Ophthalmol Vis Sci*. 2005;46(12):4536-4540.
 20. Chen L, Huq S, Gardner H, de Fougères AR, Barabino S, Dana MR. Very late antigen 1 blockade markedly promotes survival of corneal allografts. *Arch Ophthalmol*. 2007;125(6):783-788.
 21. Albuquerque RJ, Hayashi T, Cho WG, et al. Alternatively spliced vascular endothelial growth factor receptor-2 is an essential endogenous inhibitor of lymphatic vessel growth. *Nat Med*. 2009;15(9):1023-1030.
 22. Schacht V, Dadras SS, Johnson LA, Jackson DG, Hong YK, Detmar M. Up-regulation of the lymphatic marker podoplanin, a mucin-type transmembrane glycoprotein, in human squamous cell carcinomas and germ cell tumors. *Am J Pathol*. 2005;166(3):913-921.
 23. Vassar R, Rosenberg M, Ross S, Tyner A, Fuchs E. Tissue-specific and differentiation-specific expression of a human K14 keratin gene in transgenic mice. *Proc Natl Acad Sci U S A*. 1989;86(5):1563-1567.
 24. Bertozzi CC, Schmaier AA, Mericko P, et al. Platelets regulate lymphatic vascular development through CLEC-2-SLP-76 signaling. *Blood*. 2010;116(4):661-670.
 25. Patnaik SK, Stanley P. Lectin-resistant CHO glycosylation mutants. *Methods Enzymol*. 2006; 416:159-182.
 26. Kaneko M, Kato Y, Kunita A, Fujita N, Tsuruo T, Osawa M. Functional sialylated O-glycan to platelet aggregation on Aggrus (T1alpha/Podoplanin) molecules expressed in Chinese hamster ovary cells. *J Biol Chem*. 2004;279(37):38838-38843.
 27. Kingsley DM, Kozarsky KF, Hobbie L, Krieger M. Reversible defects in O-linked glycosylation and LDL receptor expression in a UDP-Gal/UDP-GalNAc 4-epimerase deficient mutant. *Cell*. 1986; 44(5):749-759.
 28. Cursiefen C, Maruyama K, Jackson DG, Streilein JW, Kruse FE. Time course of angiogenesis and lymphangiogenesis after brief corneal inflammation. *Cornea*. 2006;25(4):443-447.
 29. Zimmer G, Oeffner F, Von Messling V, et al. Cloning and characterization of gp36, a human mucin-type glycoprotein preferentially expressed in vascular endothelium. *Biochem J*. 1999;341(Pt 2): 277-284.
 30. Scholl FG, Gamallo C, Vilar S, Quintanilla M. Identification of PA2.26 antigen as a novel cell-surface mucin-type glycoprotein that induces plasma membrane extensions and increased motility in keratinocytes. *J Cell Sci*. 1999; 112(Pt 24):4601-4613.
 31. Kato Y, Fujita N, Kunita A, et al. Molecular identification of Aggrus/T1alpha as a platelet aggregation-inducing factor expressed in colorectal tumors. *J Biol Chem*. 2003;278(51):51599-51605.
 32. Ettinger R, Browning JL, Michie SA, van Ewijk W, McDevitt HO. Disrupted splenic architecture, but normal lymph node development in mice expressing a soluble lymphotoxin-beta receptor-IgG1 fusion protein. *Proc Natl Acad Sci U S A*. 1996;93(23):13102-13107.
 33. Karpanen T, Wirzenius M, Mäkinen T, et al. Lymphangiogenic growth factor responsiveness is modulated by postnatal lymphatic vessel maturation. *Am J Pathol*. 2006;169(2):708-718.
 34. Luthje K, Cramer SO, Ehrlich S, et al. Transgenic expression of a CD83-immunoglobulin fusion protein impairs the development of immune-competent CD4-positive T cells. *Eur J Immunol*. 2006;36(8):2035-2045.
 35. Mäkinen T, Jussila L, Veikkola T, et al. Inhibition of lymphangiogenesis with resulting lymphedema in transgenic mice expressing soluble VEGF receptor-3. *Nat Med*. 2001;7(2):199-205.
 36. Purpura KA, George SH, Dang SM, Choi K, Nagy A, Zandstra PW. Soluble Flt-1 regulates Flk-1 activation to control hematopoietic and endothelial development in an oxygen-responsive manner. *Stem Cells*. 2008;26(11):2832-2842.
 37. Senn KA, McCoy KD, Maloy KJ, et al. T1-deficient and T1-Fc-transgenic mice develop a normal protective Th2-type immune response following infection with *Nippostrongylus brasiliensis*. *Eur J Immunol*. 2000;30(7):1929-1938.
 38. Tomioka Y, Morimatsu M, Amagai K, et al. Fusion protein consisting of the first immunoglobulin-like domain of porcine nectin-1 and Fc portion of human IgG₁ provides a marked resistance against pseudorabies virus infection to transgenic mice. *Microbiol Immunol*. 2009;53(1):8-15.
 39. Yoshinaga SK, Whoriskey JS, Khare SD, et al. T-cell co-stimulation through B7RP-1 and ICOS. *Nature*. 1999;402(6763):827-832.
 40. Suzuki-Inoue K, Fuller GL, Garcia A, et al. A novel Syk-dependent mechanism of platelet activation by the C-type lectin receptor CLEC-2. *Blood*. 2006;107(2):542-549.
 41. Abtahian F, Guerriero A, Sebzdá E, et al. Regulation of blood and lymphatic vascular separation by signaling proteins SLP-76 and Syk. *Science*. 2003;299(5604):247-251.
 42. Fu J, Gerhardt H, McDaniel JM, et al. Endothelial cell O-glycan deficiency causes blood/lymphatic misconnections and consequent fatty liver disease in mice. *J Clin Invest*. 2008;118(11): 3725-3737.
 43. Levi M, Ten Cate H. Disseminated intravascular coagulation. *N Engl J Med*. 1999;341(8):586-592.
 44. Kyrle PA, Minar E, Bialonczyk C, Hirschl M, Weltermann A, Eichinger S. The risk of recurrent venous thromboembolism in men and women. *N Engl J Med*. 2004;350(25):2558-2563.
 45. Marenberg ME, Risch N, Berkman LF, Floderus B, de Faire U. Genetic susceptibility to death from coronary heart disease in a study of twins. *N Engl J Med*. 1994;330(15):1041-1046.
 46. McRae S, Tran H, Schulman S, Ginsberg J, Kearon C. Effect of patient's sex on risk of recurrent venous thromboembolism: a meta-analysis. *Lancet*. 2006;368(9533):371-378.
 47. Rothwell PM, Coull AJ, Silver LE, et al. Population-based study of event-rate, incidence, case fatality, and mortality for all acute vascular events in all arterial territories (Oxford Vascular Study). *Lancet*. 2005;366(9499):1773-1783.